FUDMA Journal of Renewable and Atomic Energy (FJoRAE)
ISSN: 3027-2335
Vol. 1 No 1, March 2024. Pp 1-16.

https://doi.org/10.33003/fjorae.2024.0101.01

Device Simulation Of Free Hole Transport Layer (FHTL) Based On $FASnI_3$ Perovskite Solar Cell With C_{60} Electron Transport Layer (ETL)

P. J. Manga,[1*] R.O. Amusat,[1] M. Mohammed,[2] H. Samaila, [3] E.W. Likta,[4] G. Ibrahim,[5] S. Daniel[6], N. S. Gin[7]**

[1* 3,4&5]Department of Physics, University of Maiduguri, Borno State, Nigeria.
[2]Department of Chemical Engineering, Ramat Polytechnic Maiduguri, Borno State, Nigeria
[6]Department of Science Laboratory Technology, Abubakar Tatari Ali Polytechnic, Bauchi State, Nigeria.
[7]Department of Chemistry, Federal University Gashua, Yobe State, Nigeria.

*** Corresponding author email**: 2016peterjohn@unimaid.edu.ng[1*],

Abstract

In this study, we performed device simulation for free hole transport layer (FHTL) perovskite solar cells based on $FASnI_3$ with C_{60} electron transport layer (ETL) to investigate the impact of the light absorbing layer on the performances of the proposed device. This layer is responsible for photon's absorptions and generation of charge carriers. The proposed solar cells (Glass $/FTO/FASnI_3$ $(Perovskite)/C_{60}$ $(ETL)/Au$) have been computed and simulated using a one-dimensional solar capacitances simulator (1D – SCAPS software) governed by Poisson's and continuity equations. The results of designed parameters obtained from experimental and theoretical reported works were employed during the simulation process for the proposed solar cell and the calculated optimized power conversion efficiency (PCE) of the perovskite solar cells is 17.38 (%) when compared with experimental work with power conversion efficiency (PCE) of 11.4 %. The effect of the light absorbing layer was analyzed based on varying layer thickness, defect density and band gap with an optimized open circuit voltage (V_{oc}) of 0.95 (V), close circuit current (J_{sc}) of 24.19 (mA/cm^2), Fill factor (FF) of 77.63 (%) and PCE of 17.38 (%). The results of the study give tin-based perovskite solar cells more strong hold if adopted in the design of Photovoltaic modules and thin film technology, due to their high estimated power conversion efficiency and fill factor with almost zero environmental effect than a perovskite solar cells designed based on lead.

Keywords: Perovskite solar cells, formamidinium tin iodide and 1D – SCAPS

1. Introduction

Device simulation is a powerful tool in the field of photovoltaics, allowing researchers to model and analyse the behaviour of solar cells under various conditions (Tonui *et al.,* 2018). In the context of FASnI3-based perovskite solar cells with a C_{60} electron transport layer (ETL) and a free hole transport layer (FHTL), device simulation becomes

instrumental in understanding and optimizing the performance of solar cells. Perovskite solar cells have emerged to be suitable for next-generation photovoltaic technology (Saith, 2018). They are known for their ease of fabrication, tunable optoelectronic properties, and potential for high efficiency (Kim *et al.,* 2020).

Organometal lead halide perovskite solar cells have emerged as the fourth generation of photovoltaics technology within the shortest time said to have high power conversion efficiency (PCE), thus, giving it a stronghold among competitors such as Silicon-based solar cells (Akhiro *et al.,* 2009; NREL, 2020; Schileo *et al.,* 2021). Despite having a high-power conversion efficiency (PCEs) of lead-based perovskite solar cells, most of the experiment works reported show that for both lead and tin – based perovskite solar cells have (PCEs) value less than 20%. On this note, we introduced solar capacitance simulator to optimize the experimental works as shown in tables 1 and 2 for a tin-based perovskite solar in improved it power conversion efficiency as well as fill factor. On the other hand, lead-based perovskite solar cells said to be a toxic metal which is hazardous to human life and its environs (Konstatakou *et al.,* 2017).

This environmental effect called for the replacement of lead from organometal halide perovskite with some non-toxic element. On these notes, many technologists, engineers and scientists are putting efforts to replace lead with some non-toxic element in perovskite solar cells (Zhag *et al.*, 2018; Shi *et al.,* 2017; Noel *et al.,* 2014). Some of the non-toxic elements Ge (II), Cu (I), Sn (II) and Bi (III) have been investigated and found suitable to substitute lead in perovskite solar cells (Lin *et al.,* 2019). On the same note, Sn (II) have shown to be the most promising replacement for lead because of its similar electronic properties being a member of the same group in the periodic table. Therefore, a solar cell based on Sn – perovskite rapidly degraded when exposed to a certain atmospheric condition (Gu *et al.,* 2018)

In most cases, many researchers used $CH_3NH_3SnI_3$ known as ($MASnI_3$) as an active layer in perovskite solar cells, similarly, highly efficient tin-based perovskite solar cells employed formamidinium tin iodide known as ($CH_4N_2SnI_3$ ($FASnI_3$)) which act as an active layer in tin-based perovskite solar cells (Jakar *et al.,* 2019). Due large ionic size of ($FA(CH(NH_2)_2)$ is associated with weak antibonding coupling between Sn – 5s and 1 – 5p orbitals in ($FASnI_3$) as compared with ($MASnI_3$) structure despite the tunable conductivity of $FASnI_3$. From the Milot group (2016), it has been reported that $FASnI_3$ exhibit high carrier mobility with Auger recombination with a strong radiating bi-molecular recombination rate constant as compared to $MASnI_3$ (Jakar *et al.,* 2019). Koh *et al.* (2015) reported their research on perovskite solar cells based on $FASnI_3$ with a power conversion efficiency of 1.41%. All the required techniques for boosting the efficiency of lead-based perovskite solar cells were employed in Sn-based counterparts. More so, to alleviate oxidation of SnX_2 source from Sn_4^+ ions to Sn_2^+ in the presence of air will result in poor performance of the device, Wu *et al.* (2020) added to Sn powder to SnI_2 led to the reduction of Sn_4^+ ions to $Sn_2^+$and thus, gives out maximum power conversion efficiency (PCE) of in p-i-n architecture of $FASnI_3$based solar cells. Figure 1 presents the structure of $FASnI_3$ solar cells and energy band gap

ISSN: 3027-2335

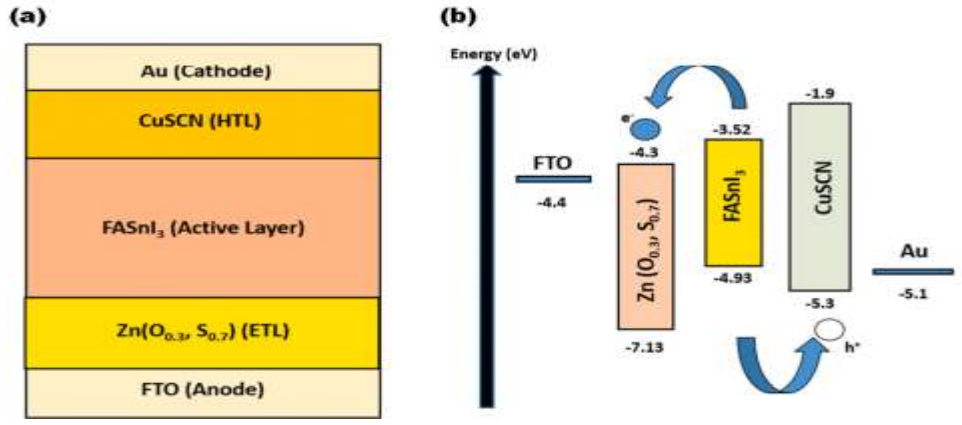

Figure 1: Structure of $FASnI_3$ solar cells and energy band gap (Wang *et al.,* 2020)

From the report of Abdelaziz *et al.* (2020), reported exceptional power conversion efficiency of 10.1% when $\pi -$ conjugate is introduced, Lewis's base molecules in controlling grain boundaries during crystallization of $FASnI_3$ films and the resulting solar cells employed ITO/PEDOT: PSS/$FASnI_3$ / C_{60}/BCP/Ag structure. Dixit *et al.* (2019) conducted experimental work using poly (ethylene-co-vinyl acetate) as an anti-solvent in the process of $FASnI_3$ film deposition, which was achieved at a power conversion efficiency (PCE) of 7.72% span for seven hours (7 hrs), simultaneously a stability was recorded at about 62.4% after forty-eight hours (48 hrs) of storage under room temperature. The recent research work of the Liu *et al.* (2020) have reported a recorded efficiency of 11.4% through the use of Phenyl-hydrazine hydrochloride (PHCl) into $FASnI_3$ films in a way to prevents the formation of Sn_4^+ions, which is reduced further through degradation of the device and results into the remaining 100% of its initial power conversion efficiency (PCE) for 100 days in a glove box (Wang *et al.,* 2020; Milot *et al.,* 2016; Liu *et al.,* 2020). This research development implies a desirable future of stable and lead-free perovskite solar cells, apart from all these experimental studies, computational studies were also used to explore another novel possibility for tin-based perovskite solar cells (Liu *et al.,* 2020) have reported an efficiency of 14.03% based on $FASnI_3$ as the active layer, TiO_2 as electron transport layer (ETL) and spiro-OMeTAD as hole transport layer using SCAPS – 1D (Kumar *et al.,* 2020).

Lucija *et al.* (2016) employed FTO/NiO/ $FASnI_3$ /C60/Au architecture for obtaining optimized power conversion efficiency of 9.99%. Stuckelberger *et al.* (2016) revealed defect density at the HTL/$FASnI_3$ interface and doping density were essential for efficient perovskite solar cells at a maximum power conversion efficiency of 9.75% at 300 nm of active layer thickness. Recently, Sharbati *et al.* (2019) have reported an optimized power conversion efficiency (PCEs) of 19.08% in $FASnI_3$-based solar cell devices with TiO_2 as ETL and spiro-OMeTAD as HTL. Madhavan *et al.* (2019) have numerically investigated $CH_3\ NH_3PbI_3$ based device using SCAPS – 1D software and studied the impact of different ETLs (TiO_2, ZnO, $Zn\ (0.03, S_{0.7})$) and HTLs (Cu_2O, $NiO, CuSCN, CsSnI_3$) on the electrical parameters performances of the device (Abdy *et al.*, 2019). In their research, they have concluded that $Zn\ (0.03, S_{0.7})$ is a desirable ETL as a replacement for TiO_2. The optimized parameters exhibit a power conversion efficiency (PCE) of 21.17%. $ZnO_{1-x}S_x$ was deposited through

ISSN: 3027-2335

the chemical bath deposition method has given out high efficiency in CIGS solar cells (Abdy *et al.*, 2019).

2. Materials and Methods

In the present work, we have investigated the simulation of $FASnI_3$ perovskite solar cell based on C_{60} as an electron transport layer (ETL) with free hole transport layer (FHTL) governed by poisson's equations and continuity equations. The simulation study was carried out through SCAPS (Version 3.3.09) software under AM 1.5G illumination. SCAPS is a 1D-dimensional widely used simulation software based on Continuity and Poisson's equations concept, developed by Prof. Marc Burgelman from the University of Gent, Belgium (Hima *et al.*, 2019; Sherkar *et al.*, 2017; Gu *et al.*, 2017; Abate *et al.*, 2013). The impact of different thicknesses and defect density of the absorbing layer for the proposed solar cell parameters have been investigated. It was found that the defect density strongly affects the power conversion efficiency (PCE), field factor (FF), open circuit voltage (V_{OC}) and short circuit current (J_{SC}). Besides, the electron affinity and doping density of ETL enhance the stability and improve the performance of the device.

.

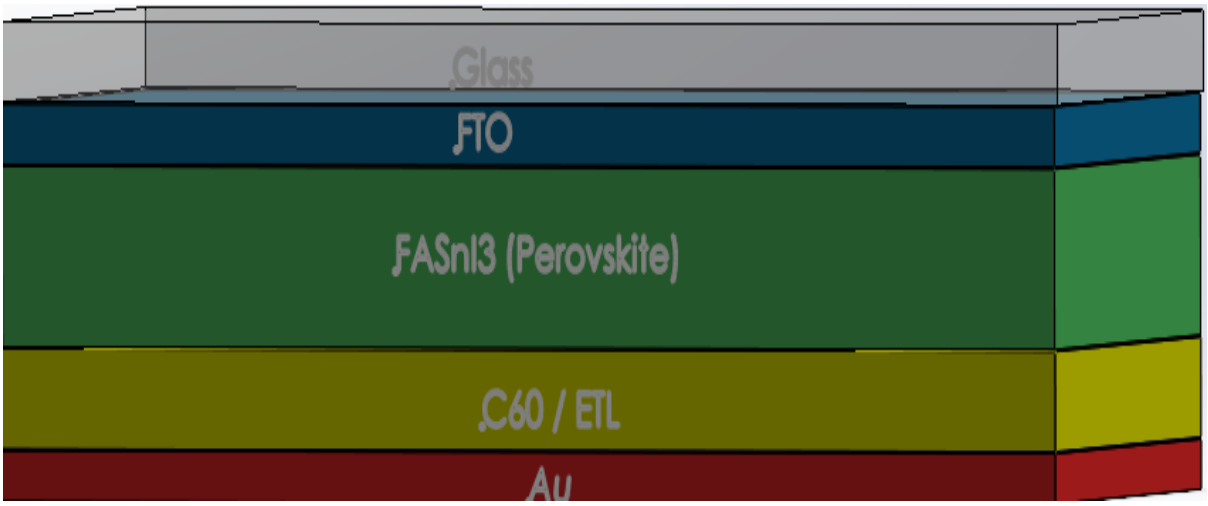

Figure 2: Proposed solar cell based on $FASnI_3$ of free Hole Transport Layer (FHTL) with Electron-Transport layer (ETL).

ISSN: 3027-2335

Table 1: Numerical parameters used in the simulation (Sherkar *et al.,* 2017; Gu *et al,* 2017; Abate *et al.,* 2013)

Parameters	C_{60}(ETL) Layer	$FASnI_3$ (Perovskite)	FTO Layer
Thickness (nm)	0.030	0.400	0.500
Band gap (eV)	1.700	1.300	3.500
Electron affinity (eV)	3.900	4.170	4.000
Dielectric permittivity (relative)	4.200	8.200	9.000
C_B effective density of states ($1/cm^3$)	8.00E+19	1.00E+18	2.2E+18
V_B effective density of states ($1/cm^3$)	8.00E+19	1.00E+18	1.8E+19
Electron thermal velocity (cm/s)	1.00E+7	1.00E+7	1.00E+7
Hole thermal velocity (cm/s)	1.00E+7	1.00E+7	1.00E+7
Electron mobility ($cm^2/v.s$)	8.00E-2	1.6E0	2.0E+1
Hole mobility ($cm^2/v.s$)	3.5E-3	1.6E0	1.00E+1
Shallow uniform donor density ND ($1/cm^3$)	0.00E+0	0.00E+0	1.00E+19
Shallow uniform acceptor density NA ($1/cm^3$)	1.00E+18	1E17	0.00E+0
Total density Nt	1.00E+15	1E16	1.00E+15

3. Results

3.1 *Device Structure and Energy Diagram*

The proposed structure of the perovskite solar cell is a p-i-n heterojunction in which $FASnI_3$ is sandwiched with C_{60} as an electron transfer layer (ETL) and free hole transport layer (FHTL) as shown in Figure 2 the proposed fluorine doped tin oxide (FTO) and Au and metal are the transparent front contact and back contact respectively. The layer configuration of the proposed device is $glass\ substrate\ FTO/FASnI_3/C_{60}/Au$. The light incident on the absorbing layer creates an electron in the valence band which absorbs energy from a photon to become a conduction band (mobile) electron both the electron as well as the hole "left behind" in the valence band said to participate in an electric current (Sherkar *et al.,* 2017). Within the absorbing layer its results into the formation of electron–hole pairs. The electrons generated are injected into the C_{60} layer because the conduction band is lower than the LUMO energy level of the absorb layer. Later the electron will be injected into FTO which tends to flow finally through the outside circuit and the holes generated in the absorbing (active) layer travel through $the\ C_{60}$ layer and reach the Au metal contact at 300K after the simulation was performed as recorded in Table 1 and Table 2, the solar cell output parameters have been obtained as follows:

ISSN: 3027-2335

Table 2: Defect density values inside the active layer and at the interface of the device simulation (Sherkar *et al.,* 2017; Gu *et al.,* 2017; Abate *et al.,* 2013).

Parameter	$FTO/FASnI_3$	$FASnI_3/C_{60}$(ETL)
Defect density	Neutral	Neutral
Capture cross section for electron (cm^2)	1.00E-15	1.00E-15
Capture cross section for hole (cm^2)	1.00E-15	1.00E-15
Energetic distribution	Single	Gaussian
Energy level concerning Ev	0.60	0.65
Characteristic energy (eV)	NA	1.00E+19
Total density (cm^{-3})	1.00E+18	1.00E+18

The proposed structure has been simulated using SCAPS-1D by obtaining research basic parameters from theoretical and experimental research papers. These parameters are E_g (energy bandgap), ϵ_r (relative permittivity), x (electron affinity), μ_n (electron mobility), μ_p (hole mobility), N_t (defect density), N_c (Conduction band effective density of states) and N_v (valence band effective density of state) which are all listed in Table 1 (Sherkar *et al.,* 2017; Gu *et al,* 2017; Abate *et al.,* 2013). The assumed thermal velocity for both electron and hole is 1.00E+7 (cm/s) while tunnelling of the interface traps has been ignored in the simulation. More so, apart from the parameters mentioned in Table 1. The defect density absorbing layer/ETL and absorbing layer (active layer)/FTO. Plays a significant role in the performance of the device, since charge carriers are generated within the layer, as given in Table 2. Furthermore, the wave function of the front contact (FTO) has been chosen as 4.4 eV and that of the back contact (Au) as 5.1 eV (Hima *et al.*, 2019) Simulation of the solar cell structural device has been carried out at illumination of AM 1.5G with an incident power of 100 $mWcm^{-2}$ at a simulated temperature of 300K, after following the condition of simulation as shown in Table 1 and Table 2. The output power of the solar cells is given as follows: $V_{OC} = 0.951176\,Volt$, $J_{SC} = 24.19\,mAcm^{-2}$, $FF = 77.63\,\%$ and $PCE = 17.378\,\%$. These simulation results were compared with available literature in both experimental and theoretical studies of $FASnI_3$ as shown in Table 3**.** The simulated output parameters are in close agreement with the previous report of theoretical and experimental works (Madhavan *et al.,* 2019). The external quantum efficiency (EQE) corresponding and J-V characteristics curves for the proposed structure have been displayed in Figures 3 and 4. Respective and are consistent with the previous reports' works (Jokar *et al.,* 2019; Wu *et al.,* 2020; Koh *et al.*, 2015; Bansal *et al.,* 2016).

ISSN: 3027-2335

Table 3: Output parameters for experimental, simulation report, simulation with hole and free hole transport layer layer (Wu *et al.,* 2020; Koh *et al.,* 2015; Bansal *et al.,* 2016).

Parameter	Experimental (18)	Simulation report (22)	Simulation Results of $FASnI_3$with HTL	Initial Simulation Results of $FASnI_3$ *without* HTL
V_{OC} (V)	0.76	1.81	0.76	0.95
J_{SC} (mAcm^{-2})	23.5	31.20	24.19	24.19
FF (%)	64	33.72	77.63	77.63
PCE (%)	11.4	17.08	14.46	17.38

3.2 Simulation Results of Current Density and Voltage of the Perovskite Solar Cells.

The simulation results of $FASnI_3$ solar cells based on I-V characteristics show that the maximum current density is recorded as 25.0 mA/cm^2 at $0.6 - 0.8$ (V) while its lowest value is recorded as $-25.0\ mA/cm^2$ at $0 - 0.2$ (V). Similarly, in Figure 2 at a wavelength of 300 – 450 nm the highest quantum efficiency is given as 85 (%) while at a wavelength of 800 – 900nm the lowest quantum efficiency is recorded as 30 (%)

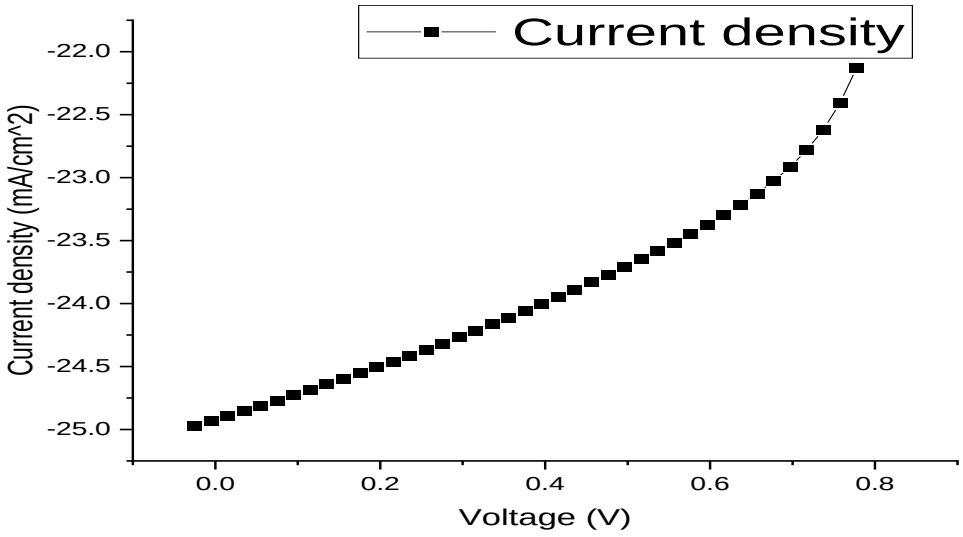

Figure 3*:* Initial simulation for I-V characteristics of $FASnI_3$ perovskite solar cells

ISSN: 3027-2335

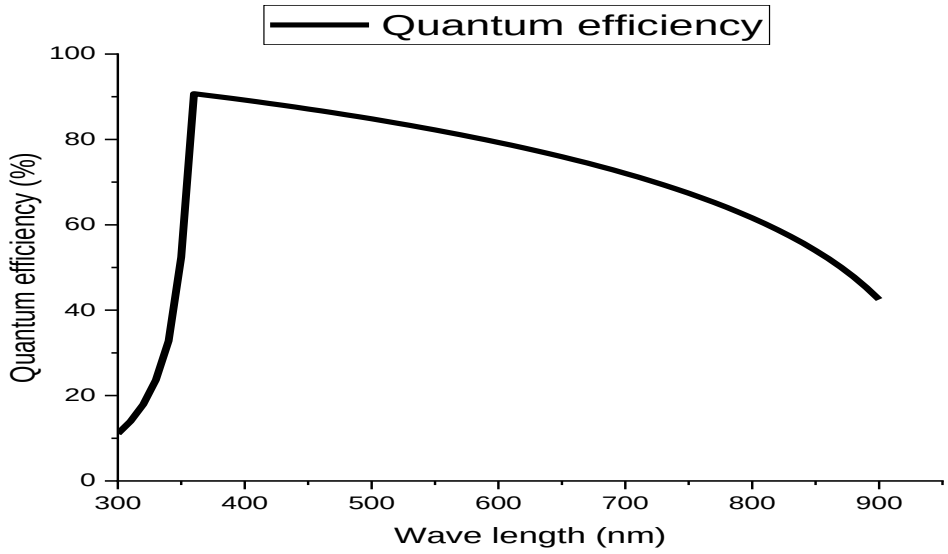

Figure 4*:* Initial simulation for quantum efficiency against wavelength of the perovskite solar cells.

3.3 Impact of the Thickness of the Active Layer

The perovskite solar cells' absorbing layer thickness plays an important role in determining the performance of the output parameter of solar cells. First and foremost, the selected absorbing material ($FASnI_3$) must be able to excite electrons from thermal equilibrium upon absorption of photons (Noel *et al.,* 2014). The light absorbing layer thickness is taking within the range of 1.0 nm – 3.5 nm for free hole transmission layer (FHTL) perovskite solar cells based on $FASnI_3$ with electron transmission layer (ETL) as shown in table 1 and table 2. The simulated results were also presented in Figures (5 and 6), this implies that there is good agreement existing between the output parameters and the layer thickness. That, as the thickness increases to some extent, the output parameters decrease in open circuit voltage, short circuit current, fill factor and power conversion factor. In all cases at 2.5 nm the maximum recorded values for V_{oc} = 0.9633 volts, $J_{sc} = 26.17\ mA/cm^2$, $FF = 77.36\ \%$ and $PCM = 18.24\ \%$ respectively.

ISSN: 3027-2335

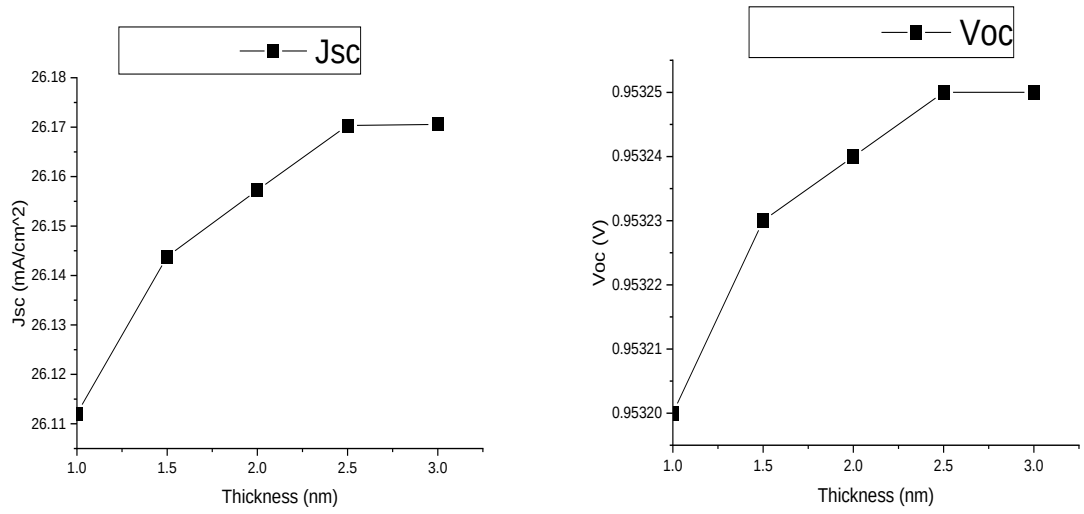

Figure 5: Batch simulation for thickness against short circuit current and open circuit voltage.

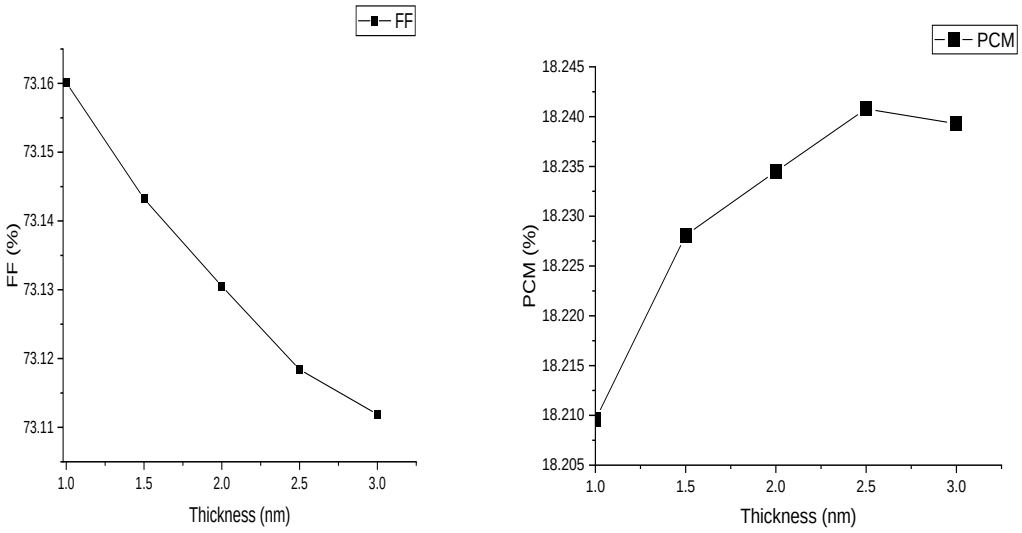

Figure 6: Batch simulation for thickness against fill factor and power conversion efficiency

3.4 Impact of band gap on the light absorbing layer (perovskite solar cells)

Solar cells consist of a potential energy barrier within a semiconductor material that is capable of separating the electrons and holes that are generated by the absorption of light within the semiconductor. In the course of our studies direct bandgap was used and found to be suitable for a small amount of materials (thin film) can be fulfill the necessity of strong absorption and help in determined the part of the solar spectrum that the material absorbed. On the same note, the lower the bandgap materials they are said to

ISSN: 3027-2335

be more suitable for low energy photon absorption which in turn improve the performance of the perovskite solar cells (Lin *et al.,* 2019; Zhang *et al.,* 2018; Shi *et al.,* 2017). The designed solar cells displayed a good relationship between the output parameters and the simulated band gap. That is, as the band gap increases the output parameter decreases. This shows that at a band gap of $1.2 - 1.6\ (eV)$, the electron is said to be sufficient to excite from its valences band to the conduction band in other to participate in conduction. Similarly, at $19 - 22\ (eV)$ there is a large difference between the valence band and the conduction band and in this case, there is no electron and energy stay between the conduction and valence band this is referred to as the forbidden energy gap. Figures (7 & 8) show that the power conversion efficiency (PCE) is maximum at $1.2 - 1.6\ (eV)$ with a recorded value of (17.8 %) and the lowest is recorded as a forbidden band by $20 - 22\ (eV)$ at a value of 4 – 14 (%), while the fill factor has its maximum recorded as 75.9 (%) at 15 (eV) and the lowest is recorded as 73 (%) at 22(eV). The results of the I-V characteristics as shown in Figure 8 display a trend as the open circuit voltage increases the current decreases. The maximum open circuit voltage is recorded at $20 - 22\ (eV)$ and the maximum current is recorded at $1.2 - 1.6\ (eV)$ respectively.

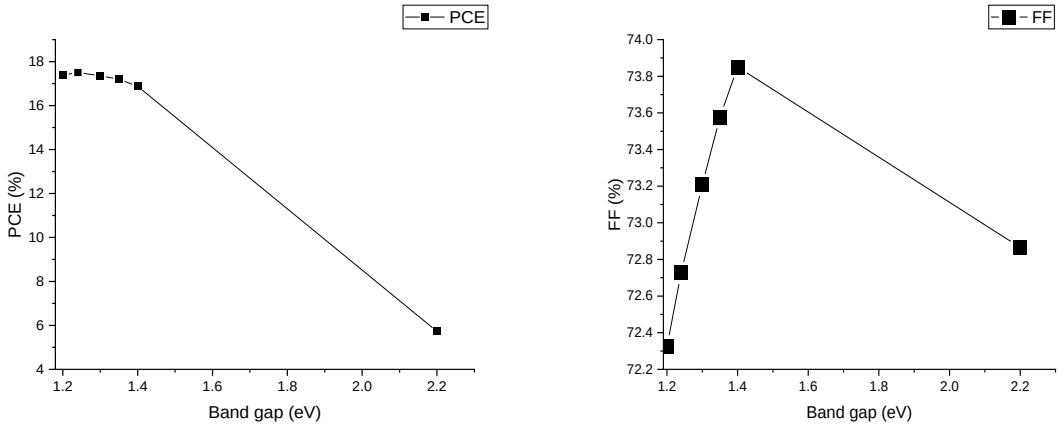

Figure 7: Batch simulation for band gap against power conversion efficiency and fill factor

ISSN: 3027-2335

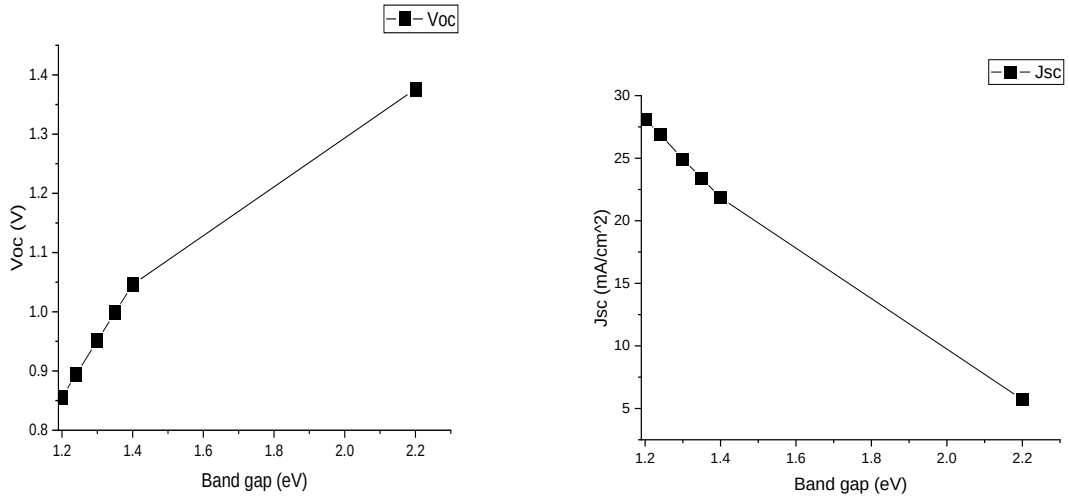

Figure 8: Batch simulation for band gap against open circuit voltage and short circuit **current**

3.5 *Impact of defect density on the light absorbing layer*

From the literature it was shown that the defect density of $FASnI_3$ layer results in recombination which is called Trap–Assisted Shock-ley-Read-Hall (SRH) (Abete *et al.,* 2013). This can be expressed by the given equations below. On the same note, N_t and E_t are the defect concentration and energy level respectively. Where σ is the cross-section of carriers and V_{th} is thermal velocity as shown in Table 1.

$$R^{SRH} = \frac{np - n_i^2}{\tau_p(n + n_i) + \tau_n(p + p_i)} \quad (1)$$

$$\tau = \frac{1}{\sigma(V_{th}N_t)} \quad (2)$$

The path travelled (distance covered) by charge carriers before they recombine in an active layer is called carrier diffusion length (L) and can be deduced using the equation below (Kim *et al.,* 2020).

$$L = \sqrt{D \times \tau} \quad (3)$$

Where is the diffusion coefficient which can be deduced by the given equation (Snaith *et al.,* 2018)

$$D = \frac{K_B T}{q} \times \mu \quad (4)$$

Where μ is the carrier mobility given as 22 $cm^{22}/V.s$

ISSN: 3027-2335

$K_B = Boltzmann\ constant = 1.381\ \times 10^{-23} J/K$

$T = 300\ K$

$q = elementary\ charge = 1.6\ \times 10^{-19} C$

4. Discussion

Results of the defect density as deduced from equations (1-4) and simulated as shown in Figure 9 and Figure 10 display the same trend pattern across all the output parameters such as power conversion efficiency (%), fill factor (%), open circuit voltage (V_{oc}) (V) and close circuit current (J_{sc}). The designed solar cells' defect density is given as $1.0\ \times 10^{18} (1/cm^3)$. The power conversion efficiency (PCM) has its maximum recorded as 20.5 – 20.6 (%) at a defect density of 2.0×10^{-14} – 14.4×10^{-14} $(1/cm^3)$. Later any further increase in the total defect density will reduce the power conversion efficiency. Whereas its lowest value is recorded as 20.1 % at a defect density of $14.1\times 10^{-15} (1/cm^3)$. Similarly, the fill factor has its maximum recorded as 79.6 79.8 (%) of the solar cells at a defect density of 2.0×10^{-14} – 14.4×10^{-14} $(1/cm^3)$. While its lowest was recorded as 78.6 % at a defect density of $14.1\times 10^{-15} (1/cm^3)$.

For short circuit current (mA/cm^2) has its maximum recorded within the range of 26.18 – 26.22 (mA/cm^2) at a defect density of 2.0×10^{-14} – 14.4×10^{-14} $(1/cm^3)$ and its lowest value is recorded at a defect density of $14.1\times 10^{-15} (1/cm^3)$ respectively. More so, A recorded value of 0.986 – 0.987 (volt) for open circuit voltage of the designed solar cells at a defect density of 2.0×10^{-14} – 14.4×10^{-14} $(1/cm^3)$. On the same note, its lowest value was recorded as 0.982 (volt) at a defect density of $14.1\times 10^{-15} (1/cm^3)$. This shows that the wider the defect density the performance of the solar will be reduced.

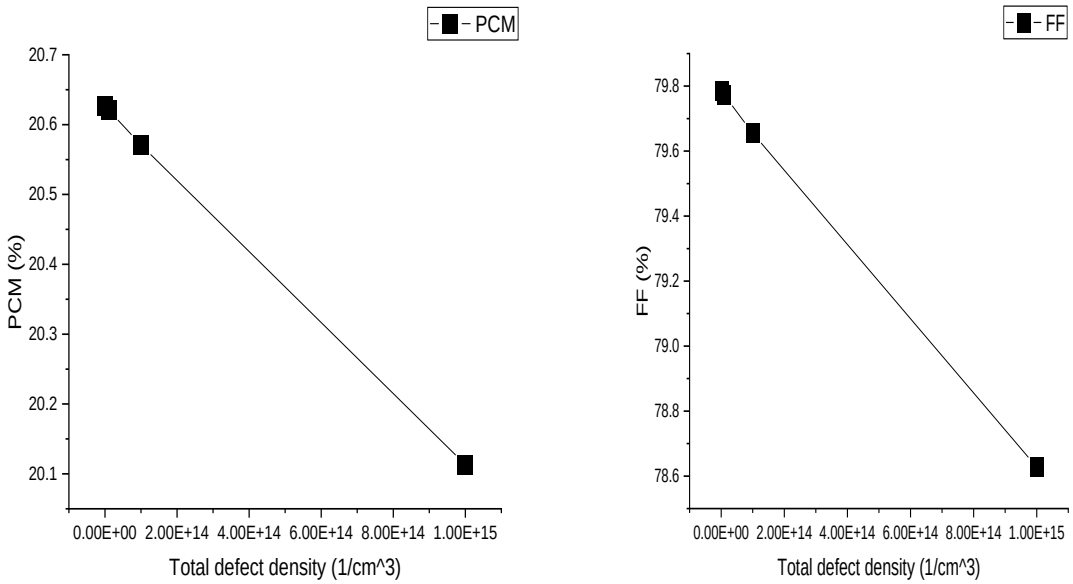

Figure 9: Batch Simulation for Total Defect Density Power Conversion Efficiency and Fill Factor

ISSN: 3027-2335

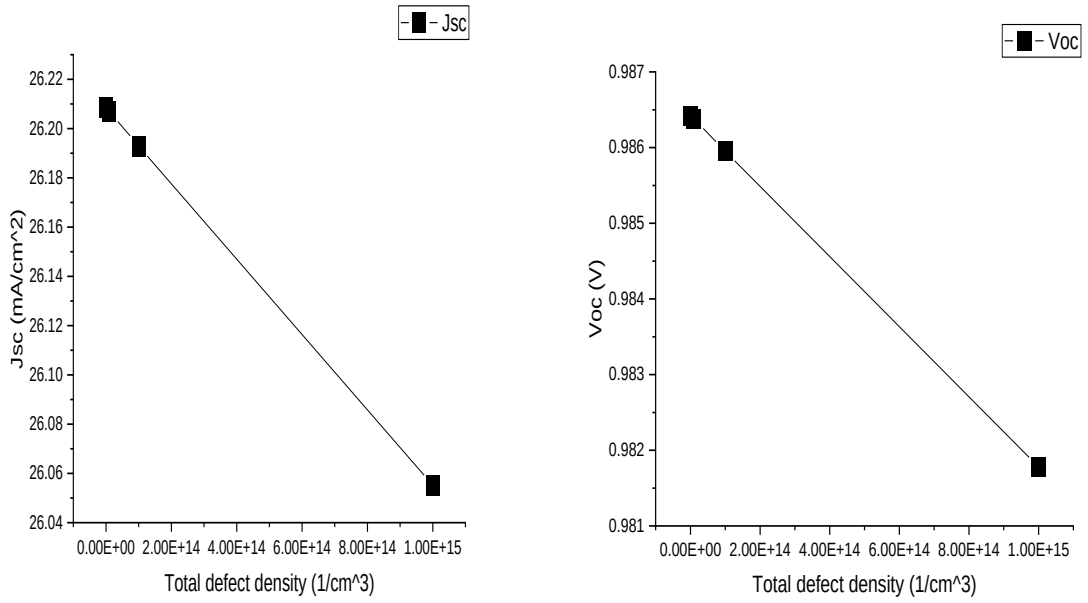

Figure 10: Batch Simulation for Total Defect Density against Short Circuit Current and Open Circuit Voltage

5. Conclusion

In recent times there have been many computational analyses and experimental studies that have been carried out on $FASnI_3$-based solar cells by many researchers. Despite the maximum value of the power conversion efficiency (PCE), $FASnI_3$-based solar cells remained below 20 (%). From our work, we were able to propose a free hole transport layer (FHTL) solar cells with a C_{60} electron transport layer (ETL) that was simulated using 1D-SCAPS. The effect of the output parameters was investigated to determine the performance of the proposed solar cell. From the simulated results when compared with other research works, it was found that the proposed free hole transport layer gives high (PCE) of 17.38 (%) than a solar cell based on a hole transport layer with (PCE) of 14.46 (%).

References

A. Abate, T. Leijtens, S. Pathak, J. Teuscher, R. Avolio, M. Errico, J. Kirkpatrick, J. Ball, P. Docampo, I. McPherson, H.J. Snaith, “Lithium salts as “redox active” p-type dopants for organic semiconductors and their impact in solid-state dye-sensitized solar cells, Phys. Chem. Chem. Phys. 15 (7) (2013) 2572–2579, https:// doi.org/10.1039/C2CP44397J.

A. Hima, N. Lakhdar, B. Benhaoua, A. Saadoune, I. Kemerchou, F. Rogti, An optimized perovskite solar cell designs for high conversion efficiency, Superlattice. Microsoft. 129 (2019) 240–246, https://doi.org/10.1016/j.spmi.2019.04.007.

ISSN: 3027-2335

C. Lin, J. Tu, X. Hu, Z. Huang, X. Meng, J. Yang, X. Duan, L. Tan, Z. Li, Y. Chen, Enhanced hole transportation for inverted tin-based perovskite solar cells with high performance and stability, Adv. Funct. Mater. 29 (2019) 1808059, https:// doi.org/10.1002/adfm.201808059.

C. Wang, F. Gu, Z. Zhao, H. Rao, Y. Qiu, Z. Cai, G. Zhan, X. Li, B. Sun, X. Yu, B. Zhao, Self-repairing tin-based perovskite solar cells with a breakthrough efficiency over 11%, Adv. Mater. (Weinheim, Ger.) 32 (31) (2020) 1907623, https://doi.org/10.1002/adma.201907623.

E. Jokar, C.H. Chien, C.M. Tsai, A. Fathi, E.W.G. Diau, Robust tin-based perovskite solar cells with hybrid organic cations to attain efficiency approaching 10%, Adv. Mater. (Weinheim, Ger.) 31 (2) (2019) 1804835, https://doi.org/10.1002/ adma.201804835.

F. Gu, S. Ye, Z. Zhao, H. Rao, Z. Liu, Z. Bian, C. Huang, Improving the performance of lead-free formamidinium tin triodide perovskite solar cells by tin source purification, Solar RRL 2 (10) (2018) 1800136, https://doi.org/10.1002/ solr.201800136.

G. Liu, C. Liu, Z. Lin, J. Yang, Z. Huang, L. Tan, Y. Chen, Regulated crystallization of efficient and stable tin-based perovskite solar cells via a self-sealing polymer, ACS applied material & interfaces 12 (12) (2020) 14049–14056, https://doi.org/ 10.1021/acsami.0c01311.

G. Schileo, G. Grancini, Lead or no lead? Availability, toxicity, sustainability and environmental impact of lead-free perovskite solar cells, J. Mater. Chem. C 9 (2021) 67–76, https://doi.org/10.1039/D0TC04552G.

H. Abdy, A. Aletayeb, M. Kolahdouz, E.A. Soleimani, Investigation of metal-nickel oxide contacts used for perovskite solar cell, AIP Adv. 9 (1) (2019), 015216, https://doi.org/10.1063/1.5063475.

H. Dixit, D. Punetha, S.K. Pandey, Improvement in performance of lead-free inverted perovskite solar cell by optimization of solar parameters, Optik 179 (2019) 969–976, https://doi.org/10.1016/j.ijleo.2018.11.028.

H.J. Snaith, Present status and prospects of perovskite photovoltaics, Nat. Mater. 17 (5) (2018), https://doi.org/10.1038/s41563-018-0071-z, 372:376.

J.Y. Kim, J.W. Lee, H.S. Jung, H. Shin, N.G. Park, High-efficiency perovskite solar cells, Chem. Rev. 120 (15) (2020) 7867–7918, https://doi.org/10.1021/acs. chemrev.0c00107.

K. Akhiro, T. Kenjiro, S. Yasuo, M. Tsutomu, Organometal halide perovskites as visible light sensitizers for photovoltaic solar cells, J. Am. Chem. Soc. 131 (2009) 6050–6051, https://doi.org/10.1021/ja809598r.

M. Burgelman, K. Decock, S. Khelifi, A. Abass, Advanced electrical simulation of thin film solar cells, Thin Solid Films 535 (2013) 296–301, https://doi.org/ 10.1016/j.tsf.2012.10.032.

M. Konstantakou, T. Stergiapolous, A critical review on tin halide perovskite solar cells, J. Mater. Chem. 5 (2017) 11518–11549, https://doi.org/10.1039/ C7TA00929A.

M. Kumar, A. Raj, A. Kumara, A. Anshul, An optimized lead-free formamidinium Sn-based perovskite solar cell design for high power conversion efficiency by SCAPS simulation, Opt. Mater. 108 (2020) 110213, https://doi.org/10.1016/j. optmat.2020.110213.

M. Nakamura, Y. Kouji, Y. Chiba, H. Hakuma, T. Kobayashi, T. Nakada, “Achievement of 19.7% efficiency with a small-sized Cu (InGa)(SeS)2 solar cells prepared by sulfurization after salinization process with Zn-based buffer, in 39th IEEE PVSC, Tampa, USA, August 2013, https://doi.org/10.1109/ PVSC.2013.6744278.

M. Stuckelberger, T. Nietzold, G.N. Hall, B. West, J. Werner, B. Niesen, C. Ballif, V. Rose, D.P. Fenning, M.I. Bertoni, Charge collection in hybrid perovskite solar cells: relation to the nanoscale elemental distribution, IEEE Journal of Photovoltaics 7 (2) (2016) 590–597, https://doi.org/10.1109/ JPHOTOV.2016.2633801.

N.K. Noel, S.D. Stranks, A. Abate, C. Wehrenfennig, S. Gaurmera, A. A. Haghighirad, Lead-free organic-inorganic tin halide perovskite for photovoltaic applications, Energy Environ. Sci. 7 (9) (2014) 3061–3068, https://doi.org/ 10.1039/C4EE01076K.

NREL (National Renewable Energy Laboratory) is the best research-cell efficiency chart. https://www.nrel.gov/pv/cell-efficiency.html, 2020.

P. Tonui, S.O. Oseni, G. Sharma, Q. Yan, G.T. Mola, Perovskite photovoltaic solar cells: an overview of current status, Renew. Sustain. Energy Rev. 91 (2018) 1025–1044, https://doi.org/10.1016/j.rser.2018.04.069.

Q. Zhang, F. Hao, J. Li, Y. Zhou, Y. Wei, H. Lin, "Perovskite solar cells: must lead be replaced–and can it be done? Science and Technology of Advance Materials 19 (2018) 425–442, https://doi.org/10.1080/14686996.2018.1460176.

R. Lucija, R. Gehlhaar, T. Merckx, W. Qiu, U.W. Paetzold, H. Fledderus, J. Poortmans, Interconnection optimization for highly efficient perovskite modules, IEEE Journal of Photovoltaics 7 (1) (2016) 404–408, https://doi.org/ 10.1109/JPHOTOV.2016.2626144.

R.L. Milot, G.E. Eperon, T. Green, H.J. Snaith, M.B. Johnston, L.M. Herz, Radiative monomolecular recombination boosts amplified spontaneous emission in HC (NH2)2SnI3 perovskite films, J. Phys. Chem. Lett. 7 (20) (2016) 4178–4184, https://doi.org/10.1021/acs.jpclett.6b02030.

S. Abdelaziz, A. Zekry, A. Shaker, M. Abouelatta, Investigating the performance of formamidinium tin-based perovskite solar cell by SCAPS device simulation, Opt. Mater. 101 (2020) 109738, https://doi.org/10.1016/j.optmat.2020.109738.

S. Bansal, P. Aryal, Evaluation of new materials for electron and hole transport layers in perovskite-based solar cells through SCAPS-1D simulations, in IEEE 43rdPhotovoltaic Specialists Conference (PVSC), 2016, https://doi.org/10.1109/ PVSC.2016.7749702, 0747-0750.

S. Sharbati, J.R. Sites, Impact of the band offset for n-Zn(O, S)/pCu(In, Ga)Se2 solar cells, IEEE JournalJournal of Photovoltaics 4 (2) (2014) 697–702, https://doi.org/ 10.1109/JPHOTOV.2014.2298093.

T. Wu, X. Liu, X. He, Y. Wang, X. Meng, T. Noda, X. Yang, L. Han, “Efficientandstabletin-based perovskite solar cells by introducing π-conjugated Lewis base, Sci. China Chem. 63 (1) (2020) 107–115, https://doi.org/10.1007/ s11426-019-9653-8.

T.M. Koh, T. Krishnamoorthy, N. Yantara, C. Shi, W.L. Leong, P.P. Boix, A. C. Grimsdale, S.G. SMhaisalkar, N. Mathews, Formamidinium tin-based perovskite with low Eg for

ISSN: 3027-2335

photovoltaic applications, J. Mater. Chem. A 3 (29) (2015) 14996–15000, https://doi.org/10.1039/C5TA00190K.

T.S. Sherkar, C. Momblona, L. Gil-Escrig, J. Avila, M. Sessolo, H.J. Bolink, Recombination in perovskite solar cells: significance of grain boundaries, interface ChemPhysChem 18 (6) (2017) 617–625, https://doi.org/10.1002/ cphc.201601245.

V.E. Madhavan, I. Zimmermann, A.A.B. Baloch, A. Manekkathodi, A. Belaidi, N. Tabet, M.K. Nazeeruddin, CuSCN as hole transport material with 3D/2D perovskite solar cells, ACS Appl. Energy Mater. 3 (1) (2019) 114–121, https://doi. org/10.1021/acsaem.9b01692.

X. Gu, Y. Wang, T. Zhang, D. Liu, R. Zhang, P. Zhang, J. Wu, Z. David Chen, L. Shibin, Enhanced electronic transport in Fe3+-doped TiO2 for high-efficiency perovskite solar cells, J. Mater. Chem. 5 (41) (2017) 10754–10760, https://doi. org/10.1039/C7TC03845C.

Z. Shi, J. Guo, Y. Chem, Q. Li, Y. Pan, H. Zhang, Y. Xia, W. Huang, Lead-free organic-inorganic hybrid perovskites for photovoltaic applications: recent advances and perspectives, Adv. Mater. (Weinheim, Ger.) 29 (2017) 1605005, https://doi.org/10.1002/adma.201605005.